Journal of Applied Physics PERSPECTIVE scitation.org/journal/jap

Challenges, myths, and opportunities in hot carrier solar cells

Cite as: J. Appl. Phys. **128**, 220903 (2020); doi: 10.1063/5.0028981
Submitted: 8 September 2020 · Accepted: 26 November 2020 ·
Published Online: 11 December 2020

D. K. Ferry,[1,a)] S. M. Goodnick,[1] V. R. Whiteside,[2] and I. R. Sellers[2]

AFFILIATIONS

[1]School of Electrical, Computer, and Energy Engineering, Arizona State University, Tempe, Arizona 85287-5706, USA
[2]Homer L. Dodge Department of Physics and Astronomy, University of Oklahoma, Norman, Oklahoma 73019, USA

Note: This paper is part of the Special Topic on Hot Electron Physics and Applications.
[a)]**Author to whom correspondence should be addressed:** ferry@asu.edu

ABSTRACT

Hot carrier solar cells hold the promise of efficiency significantly greater than that predicted by the Shockley–Queisser limit. Consequently, there has been considerable effort to create cells that achieve this goal, but so far, this has not been realized. There are many reasons for this. Here, the principles of the concept will be discussed along with some myths that hinder the future development of such devices. Also, a new approach to the hot carrier solar cell is described along with some recent experimental results that support such an approach.

I. INTRODUCTION

The photovoltaic (PV) solar cell is one of the fastest growing renewable energy sources available today. Consequently, there is great interest in improving the technology, particularly with respect to the efficiency that can be attained in these cells. Yet, the underlying science is quite old. The photovoltaic process was originally discovered by Bequerel in 1839[1] using platinum electrodes on a silver halide.

The first solar cell was apparently developed by Fritts in 1883[2] using gold electrodes on selenium. The first p–n junction solar cell was patented in 1946[3] but was subsequently improved using Si to provide relatively efficient solar energy conversion.[4] Today, a great many materials are used in the search for even greater and more optimum efficiency.[5]

In studying diode solar cells, it is important to realize that the normal p–n junction diode operates in a dramatically different fashion than the p–n junction solar cell. The normal p–n junction diode is classically referred to as a *minority* carrier device (Fig. 1) in that carriers move from high density to low density regions when the device is turned on (V_{to}), i.e., flowing into regions in which they are the minority carriers. Under forward bias, electrons are injected into the p-region across the p–n junction and eventually recombine with the holes to provide a current. Similarly, holes are injected into the n-region and eventually combine with the electrons to contribute to the current. Note that the directions in which these minority carriers move are opposite to that if they were responding to the built-in electric field. For that reason, this electric field is generally never mentioned in discussions of the diode current.

In addition, one often associates quasi-Fermi levels (QFLs) with the bands in these normal junctions. The electron QFL is near the conduction band in the n-type material and the hole QFL is near the valence band in the p-type material. Applied bias to the device leads to a separation of these two levels given by this applied bias (with the electron QFL at a higher energy than the hole QFL).

Traditional silicon junction solar cells are considered a *minority* carrier device as well, as the photogenerated carriers diffuse to the depletion region and contribute to the current. On the other hand, advanced concept heterostructured solar cells should be considered a *majority* carrier device. Solar photons create electron–hole (e–h) pairs wherever they are absorbed throughout the device. In contrast to the normal operation of a p–n junction, usable photogenerated current occurs at voltages less than V_{to}, or, more specifically, less than the open-circuit voltage V_{OC} (the voltage at which the current is zero even under illumination).

For efficient cell operation, the carriers need to reach the junction depletion region where the electric field separates the electrons and holes. This implies that the depletion region should be as close to the illuminated surface as possible, as there is generally a significant difference in mobility of the electrons and holes necessitating

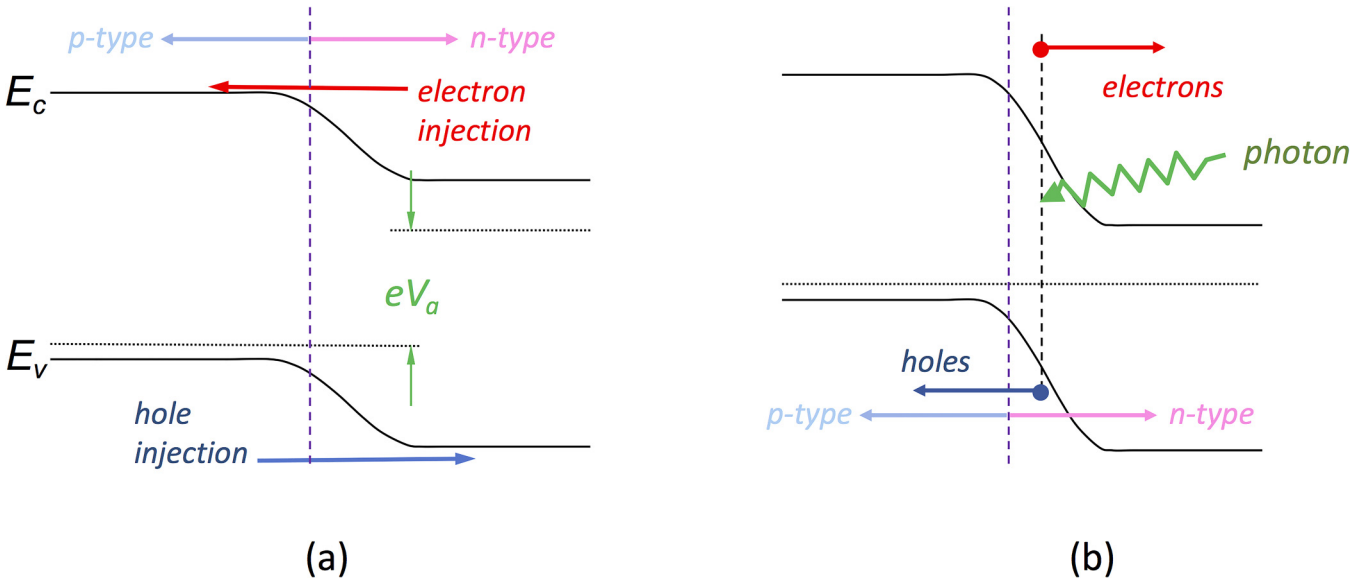

FIG. 1. (a) Carrier injection in a forward biased *p–n* junction. The injected carriers become minority carriers in the respective region. (b) The electron–hole pair created by a photon, in the depletion region, are separated by the built-in electric field and become majority carriers in their respective regions.

a differential path length to compensate for the mobility differences. This is, of course, easier to do in a III–V cell, where the absorption coefficients are much larger than in, e.g., silicon.

In the depletion region, the photoelectrons move toward the *n*-region, in response to the electric field, where they will be majority excess carriers while the holes move toward the *p*-region, in response to the electric field, where they will be majority excess carriers. These electrons and holes move to the contacts entirely as majority carriers in their respective regions, that is, they move as drift currents.[6] In these cells, the carriers move as they would in bulk majority carrier material, and the photocurrent entirely depends upon their movement in response to the electric field. This difference will be important in our subsequent discussions below.

When the electron–hole pair is formed, each particle is likely to have an energy higher than the bandgap of the host material. For example, the solar spectrum peaks at around 2.0–2.5 eV, while the typical bandgap of a commercial solar cell is around 1.0 eV, so that the electron and hole have a combined kinetic energy of some 1.0–1.5 eV. Thus, the created electron and hole have considerable excess energy, which is usually relaxed by the emission of energetic phonons with the energy going into heating of the lattice. This heat loss is a major contributor to the losses invoked in a single junction solar cell,[7] with more than half of the solar energy being lost to the lattice.[8]

In 1982, Ross and Nozik proposed that a hot carrier solar cell (HCSC) could be made that would reduce the thermal losses and provide a much higher efficiency;[9] thus, the HCSC has become a potential candidate for the so-called third generation solar cell. A review of various third generation concepts was given by Green.[10]

Ross and Nozik suggested that to achieve the predicted efficiencies, one has to achieve two objectives: (1) prevent the photo-carriers from thermalizing to the band edges by emission of optical phonons and (2) extract only the hot carriers into the contacts through an energy-selective contact. Since then, an extensive effort has been made to achieve these goals with limited success. The problem lies not in the concept but perhaps in the limited views that have been brought to the effort.

In this perspective, some of the challenges will be discussed, as well as some of the myths that have inhibited progress in HCSCs. Perhaps what is of utmost importance when considering a hot carrier solar cell is that it needs to operate in a far-from-equilibrium steady state, that is, the excited photogenerated carriers are quite likely to be in a distribution that is not of Fermi–Dirac character and may well be non-thermal in shape. Nevertheless, the distribution of the carriers in space and time is in steady state, with all flows balancing. We will discuss this further below. This will be followed by a discussion of a new approach that expands the view in a different direction.[11] Throughout, experimental data that are relevant to this new approach also will be discussed. Some of the challenges and future thoughts will be provided in the Conclusions.

II. PHYSICS OF HCSC

All electronic devices depend upon the adaptation of Maxwell's equations, which, in turn, describe the fields that arise from the relativistically invariant charge and flux, as well as the motion of these two quantities. Fortunately, for relatively low frequencies, the effects of these two quantities can be separated via the Coulomb gauge (for which, e.g., Poisson's equation lacks the time derivatives of the scalar potential's wave equation), and this allows one to concentrate upon the charge that is important in our solar devices. A voltage is created by a dipole of charge. Current is the motion of charge.

These two are the observables for our operating junction solar cell. So, the control of the charge leads to the details of the solar cell.

It is also important to understand that the solar cell, in general, and the HCSC, in particular, is a far-from-equilibrium device.[12] As such, while large photogenerated carrier concentrations can occupy the upper valleys, and define V_{OC} of such a device, these will have a rather non-thermal distribution and, therefore, one should approach defining a carrier temperature, or a quasi-Fermi level, with great care, especially in the valley photovoltaic HCSC proposed in Sec. III. Therefore, equilibrium concepts such as detailed balance[13,14] should be used with care as it may well lead to a misunderstanding of the device physics.[15] Instead, one needs to work with the conservation of charge, current, and energy, the flows of these quantities.

In the p–n junction, an n-type region is brought together with a p-type region, and the point at which they are adjoined is where the depletion charge is located. Recombination leads to the depletion of electrons in the n-region and holes in the p-region, with the uncompensated donors and acceptors producing the built-in charge and voltage (Fig. 1).

Let us consider, as a clarifying example (which we will use below as well), a p–n junction between heavily p-doped $Al_{0.48}In_{0.52}As$ and lightly n-doped $Ga_{0.47}In_{0.53}As$, which are both lattice-matched to an InP substrate. In this example, GaInAs is the top layer upon which the solar radiation will impinge. AlInAs is acceptor doped to $10^{18}\,cm^{-3}$ and the GaInAs is donor doped with $10^{15}\,cm^{-3}$. The Fermi level in AlInAs lies about 0.17 eV above the valence band, while that in GaInAs lies about 40 meV below the conduction band. This produces a built-in potential of ~0.8 V and a depletion region width of ~1.1 μm, of which almost 90% lies in GaInAs.

If the cell is built with only a 0.5 μm thick GaInAs layer, the electrostatics of the depletion region are not explicitly satisfied, but this can be solved by adding a thin, heavily n^+-doped layer on top of the GaInAs. The heavy doping will effectively terminate the depletion layer (which is discussed further below), leaving a very high electric field throughout the central GaInAs layer in this p^+–n–n+ structure. This structure is unusual for most solar cells that are typically just p–n diodes (but is closer to the p–i–n diode often used); yet, this structure is already a HCSC, for reasons that will be discussed below.

In Fig. 2, the absorption coefficient for $Ga_{0.47}In_{0.53}As$ (adapted from Adachi[16]) and the fraction of photons absorbed in this central 0.5 μm layer are shown. Notably, above 1.5 eV, nearly all the photons are absorbed. Below this energy, a significant fraction of photons are not absorbed, but these cannot be absorbed in the AlInAs layer either, because they are below the bandgap. This lack of absorption (i.e., transmission) represents a loss process that is dependent upon the thickness of the absorption layer. A thicker layer, or a backside mirror, could reduce this loss to some degree. Nevertheless, there will be some loss of low energy (long wavelength) photons, and this is an unavoidable loss in any solar cell, which becomes worse as the energy gap is increased via the use of different materials.[13]

The absorption of sunlight now leads to the excess electrons and holes, which move as discussed above. This current flow

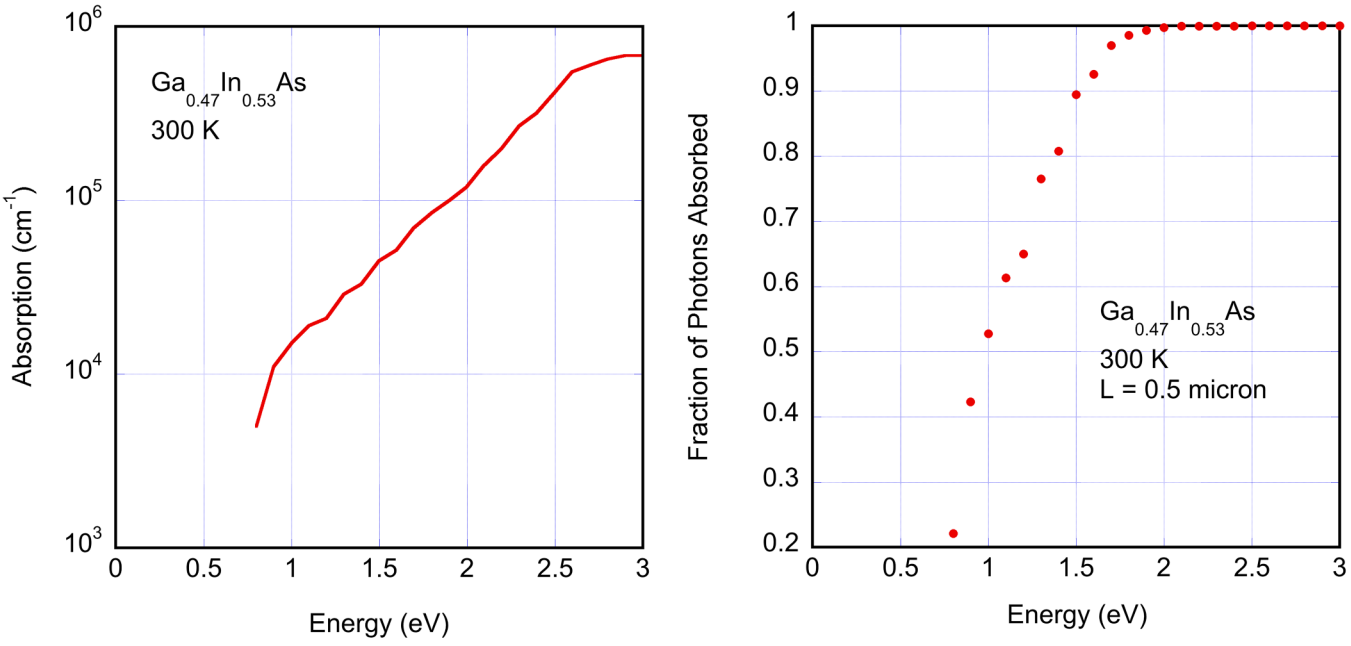

FIG. 2. (a) The absorption coefficient for $Ga_{0.47}In_{0.53}As$ at 300 K. (b) The fraction of photons that are absorbed in this material at 300 K for a 0.5 μm layer. The top surface reflection has been ignored and must be taken into account in a real cell, although there are many ways to reduce this reflection.[5]

actually reduces the built-in charge and leads to the open-circuit voltage of the cell. While there is no physical reason that the photogenerated charge cannot exceed the built-in charge, this would greatly reduce the built-in potential and its important electric field. Extracting this charge from the cell results in the photocurrent observed from the cell.

Now, let us look at the QFLs. If we have $\sim 10^{14}\,\mathrm{cm}^{-3}$ photoelectrons in the L valleys, we can perhaps assign a temperature of 500 K to these carriers (but see Sec. IV A). The bands in these valleys are germanium-like so that the effective density of states at this temperature is nearly $2 \times 10^{19}\,\mathrm{cm}^{-3}$, so that the electron QFL lies some 0.6 eV below the L valleys (actually even below the Γ valley) while the hole QFL lies an equivalent amount above the valence band in InAlAs. Hence, the splitting of the two QFLs is large and *negative*. In this situation, the QFLs are not a good indication of V_{OC}, and it would be a mistake to connect this quantity to the view of an applied bias. The ideal operation of HCSCs decouples the QFL splitting from V_{OC} and rather makes the latter dependent upon the extraction energy of the photo-carriers. The latter is correlated with the wide bandgap material where extraction occurs, not to the bandgap of the absorber material. The same concept has been pursued in both quantum well and intermediate band solar cells, so that V_{OC} may be higher than the absorber bandgap.

A. Recombination

Shockley and Queisser considered the thermodynamics of solar cells and concluded that radiative recombination would be the major loss mechanism in these devices.[13] However, this can be avoided to a large extent. To understand this, let us refer to the work of Rau that compared solar cells and light-emitting diodes (and by extension semiconductor laser diodes).[17] Of course, these light-emitting devices depend upon radiative recombination. In laser diodes, the light emission efficiency increases, and the threshold decreases, as one moves from bulk devices, to quantum well devices, to nanowires and quantum dots.[18] The reason for this is that, as one moves from 3D to 0D, the electron and hole are more closely confined, so that the likelihood of recombination increases. This means that recombination decreases rapidly with the distance between the electron and the hole.

In the structure discussed above, the photogenerated electron and hole are spatially separated due to the electric field of the depletion region. It is highly unlikely that an electron and hole, separated by hundreds of nanometers in space, will undergo recombination. In fact, this seems to be a common understanding, since recombination is likely to be second- or third-order and thus not a source of significant loss in a device, especially if the electron–hole pairs are entirely created in the depletion region.

By no means does this imply that recombination is not important in the general solar cell. First, of course, is the fact that the cell, in the absence of any solar illumination, will be in thermal equilibrium with its environment, absorbing room temperature blackbody radiation and emitting sufficient radiation of its own to reach equilibrium.

Typical III–V solar cells are heavily doped and so may be only a few micrometers thick with a depletion layer of only a few 10s of nanometers. In such cells, most of the photogenerated electrons and holes may be created in the region outside the depletion region and must diffuse to the latter region before separating, although the resulting majority carrier currents move by a drift velocity. Thus, they remain fairly close to one another and recombination is a problem. However, by keeping the junction depletion region close to the surface, the recombination loss can be minimized.

B. Phonon losses

One of the major loss processes is the emission of phonons by the photoexcited electrons and holes; the reduction of this loss was one of the issues identified by Ross and Nozik.[9] The major phonon loss in the III–V materials is the polar optical phonons, because of their Columbic characteristic.[19] In alloys, such as GaInAs, that is discussed here, this phonon can be more problematic due to its two-mode behavior; e.g., there is a GaAs-like mode and an InAs-like mode.[19] In the lattice-matched composition discussed above, the GaAs-like mode energy is 32.6 meV and the InAs-like mode is 29.1 meV.[19] To determine the coupling to each of the two modes requires full knowledge of the dielectric function in the Reststrahlen region, in order to apportion the lattice polarizability between the two modes; this is generally difficult. As a consequence, one tends to use a weighted average of these two modes together with a single 34 meV phonon (an average of the pure GaAs LO 35.41 meV and the pure InAs LO 29.6 meV).[20]

The idea of using a superlattice of materials—in which the minibands were narrower (in energy) than the LO-mode energy and the gaps were wider than the LO-mode energy in order to inhibit phonon emission—apparently originated with Sakaki,[21] although suggestions of this were observed earlier.[22] This approach has been followed by many in the HCSC field.[23] But, the use of such superlattices tends to reduce the actual volume in which photons can be absorbed effectively, although others seek to create a very non-equilibrium phonon distribution that results in a phonon bottleneck.[24]

In $Ga_{0.47}In_{0.53}As$, the scattering rate for the polar LO phonon is of the order of $4–5 \times 10^{12}\,\mathrm{s}^{-1}$.[11] Therefore—for example—considering a photon with an energy of the order of 2.0–2.5 eV, the electron and hole together will have an excess energy of 1.25–1.75 eV; the electron's share will be ∼1.2–1.6 eV in this example. In the bulk, one would then expect that the electron would then lose 34–45 phonons in equilibrating with the lattice. Hence, the electron loses almost its entire kinetic energy toward heating of the lattice. However, in our restricted structure of the cell above, this loss is affected by the velocity of the carriers.

In the diode described, the electric field is of the order of 16 kV/cm at the physical junction and ∼10 kV/cm at the heavily doped n^+ layer that terminates the depletion region. Ballistic velocities of $4–5 \times 10^7$ cm/s can be obtained in quantum wells of this material,[25,26] and the peak velocity at 2.0 kV/cm is almost 3×10^7 cm/s.[11] Thus, the average amount of time spent in the absorption region is less than a few picoseconds, which sets a time scale for the cell. Given the scattering rate above, this means that, at most, only about ten LO phonons will be lost, a fact already predicted by Ross and Nozik.[9] Nevertheless, this can be further modified, as will be discussed in Sec. III. The important

point of this discussion is that the heterostructure device described above may already be considered to be a HCSC, as the "hot" carriers will not lose the immense number of phonons expected in equilibration seen in conventional solar cells.

C. Energy filtering

While Ross and Nozik do not specifically describe using energy filters, they do specify the desire to have carriers removed at an optimum single energy.[9] However, the HCSC community has largely taken this comment to mean the use of an energy filter, such as a resonant tunneling structure through which to extract the carriers.[27] At the same time, the former authors talk about the hot carriers thermalizing among themselves to a very high effective temperature. This gives rise to another problem that, along with the complexity of implementing such systems, arises because using an energy filter on a hot carrier distribution may extract only a fraction of the carriers (we return to the thermal question in Sec. IV A).

Upon excitation of the photoexcited carriers and their movement in the applied electric field, the population is relatively non-thermal (as will be discussed in Secs. III A and IV A). Therefore, the assumption that the hot carriers generated at short times can be described by a Maxwell–Boltzmann (MB) distribution must be considered with care. While a thermal distribution is being invoked above, one cannot forget the fact that this device is a far-from-equilibrium device. If we desire that carrier–carrier scattering pushes the distribution into a thermal MB distribution, the carrier–carrier scattering rate must be much larger than all other scattering rates combined.[28] This requires a very high carrier density, which is not the case in the absorber layer. Even in Si, with a reasonably high doping, the electron–electron (e–e) scattering rate can be as small as $10^{13}\ s^{-1}$,[29] and similar rates are found in GaAs quantum wells.[30] As we discuss below, the phonon scattering that is present can form the distribution into something that resembles a thermal distribution, but it has major differences. Moreover, the idea that the narrow energy range that is extracted can be rapidly refilled from the rest of the distribution is only true on a very long time scale (>10s of ps.). If *all* of the hot carriers are not extracted on the short time scale (mentioned above), then carriers will accumulate at the n–n^+ interface, and this may lead to the formation of a high potential barrier, which tends to repel further electrons from arriving at the interface (basically, carrier–carrier repulsion).

In a HCSC, the major task of the extraction layer is to get the hot carriers out and to keep the cold carriers in—or extract such hot carriers via the high energy pathway facilitating hot carrier extraction so the voltage is defined by the high energy contact. Of course, it is preferable that a large majority of carriers are hot and a very small number are cold. As mentioned, we need all the hot carriers to be extracted on the short time scale. This can be accomplished by using a semi-infinite barrier that allows the hot carriers to pass over the top while keeping the cold carriers from leaving the device.[5,31] This can be achieved with a wide bandgap layer or even a properly chosen Schottky barrier.[32]

III. A NEW APPROACH

In the preceding discussion, only the undergraduate concept of energy bands has been used; i.e., a simple conduction and valence band in each material. However, the idea of keeping the carriers hot for the HCSC suggests that more of the real band structure should be utilized. The idea is analogous to lasers where an upper metastable energy level is used in order to build the electron density sufficient to create a population inversion. Here, upper levels of the conduction band (L or X valleys) are used to store the energetic electrons and create the envisioned population inversion.[10]

A. Valley photovoltaics

In the cell described above, the GaInAs metastable level will primarily be the L levels of the conduction band, which lie ~0.5 eV above the conduction band minimum at Γ. Energetic electrons at 1.25–1.75 eV have a much higher scattering rate to L than that of the LO phonon, so that most of the photogenerated electrons will transfer preferentially to this satellite valley. In addition, the high electric field in the GaInAs absorption layer will accelerate, and therefore also scatter, the lower energy carriers up to the satellite valley as well.

In Fig. 3, the band structure of the proposed HCSC (described above) is plotted, along with a 25 nm n^+-GaInAs layer that is grown to terminate the depletion region at the surface.[33] The surface upon which the photons impinge is on the left of this

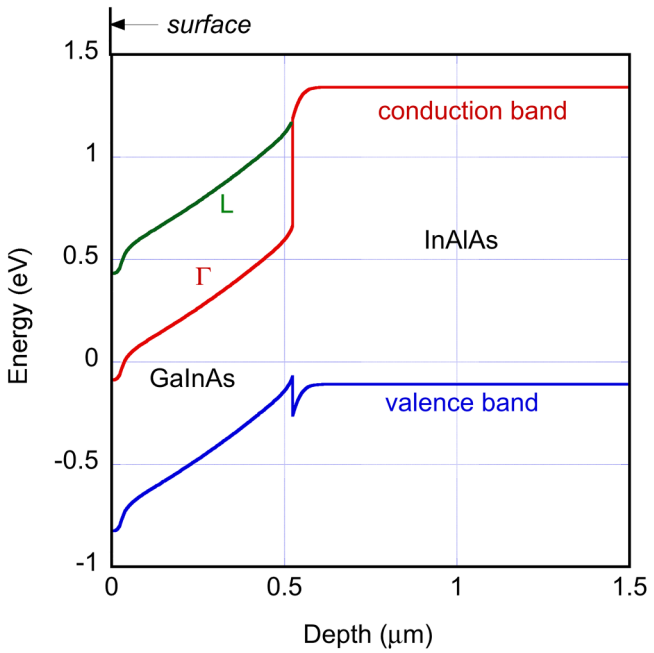

FIG. 3. The energy bands of the example structure showing the position of the L valleys in the GaInAs. In equilibrium, the Fermi level lies at $E = 0$ eV. The n-type layer is on the left, and light is assumed to enter from the left.

figure. Here, one sees that lower energy carriers need only travel ballistically to reach the upper L valleys.

To be sure, electrons in the L valleys will scatter, but the primary scattering is between equivalent L valleys, and this is done by a zone edge LA mode.[18] This mode has an energy of ~24 meV. The velocity of electrons in these valleys at high fields can be of the order of 2×10^7 cm/s in quantum well HEMTs,[26,34] but in the bulk, Monte Carlo studies suggest it is about a factor of 3 lower.[11] Nevertheless, these carriers will remain in the GaInAs only about 3 ps, so could lose little energy to these zone edge modes, but can approximate a thermal distribution (this is discussed further in Sec. IV A) within these L valleys.[11]

B. Holes

The photogenerated holes move into the *p*-type InAlAs, from the depletion region, as a majority carrier, after being accelerated by the electric field in the depletion region [see Fig. 1(b)]. However, the mobility of the holes is quite low. Experimental values for this parameter tend to be in the range of 40–75 $cm^2/V\,s$,[35] or even lower.[36] It is thought that this mobility may be limited by disorder scattering and values in high quality material may be as high as 175 $cm^2/V\,s$.[37] Even in the high field of the depletion region, this is unlikely to yield a velocity much above 10^6 cm/s. Nevertheless, this sets the hole current level throughout the InAlAs layer (due to conservation of current).

There is not much chance for recombination since the electron concentration in this *p*-type material is only about $3.4 \times 10^{-6}\ cm^{-3}$ due to the large bandgap and small intrinsic concentration. However, it is known that minority carrier injecting contacts have existed ever since semiconductors have been studied. In HEMTs, the buildup of these injected carriers can create rather high electric fields.[38] So, it is possible that the contacts may inject minority carriers and lead to recombination, but radiative recombination can lead to reabsorption of the electron–hole pair, so this does not lead to a real loss, only a translation of the pair in the device. With the low mobility, it is more likely that holes buildup just outside the depletion region and lead to a non-uniform hole density and resulting majority carrier diffusion, as well as drift.[6] No matter how the holes make it to the back contact, the properties of the InAlAs are likely to lead to non-negligible resistance in the material away from the depletion region, and this is not particularly good for achieving very high efficiencies in the device. Yet, the potential drop in this layer aids in the drift of the carriers, so some optimization is necessary in cell design.

C. Experiments

Experiments with devices in which the upper (field terminating) layer is lattice-matched n^+ AlInAs, and in which this layer also creates the energy-selective barrier, have shown that the intervalley transfer desired for these devices actually does occur, and most of the photogenerated electrons indeed occupy the L valleys.[39] Photoluminescence suggests that only a few, cooler carriers remain in the Γ valley, but the cell requires further optimization since the absorber–barrier valley degeneracy results in a barrier to efficient carrier extraction. This is illustrated in Fig. 4(a), where

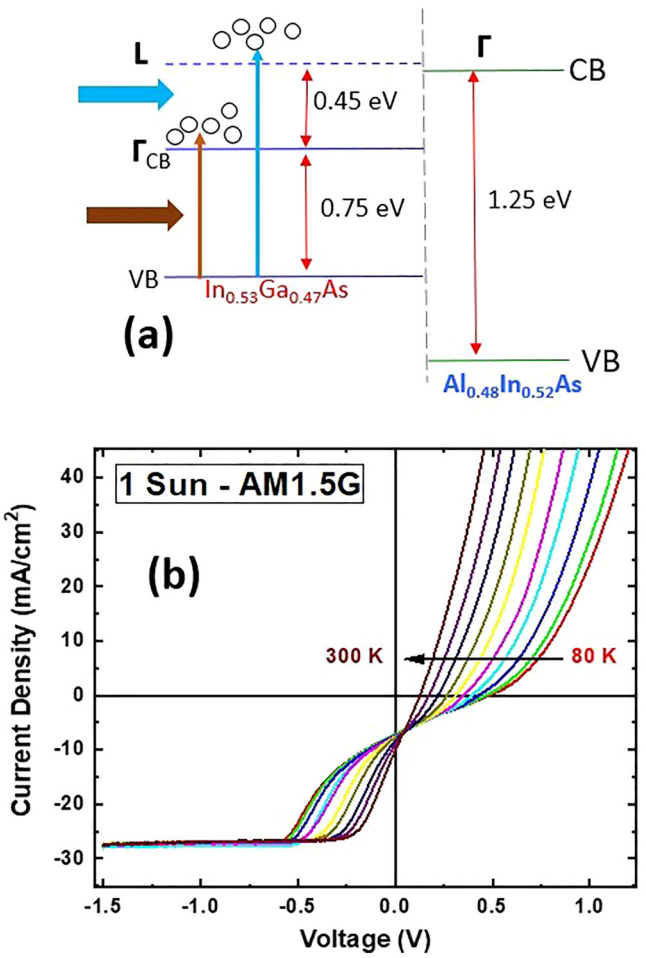

FIG. 4. (a) Schematic band alignments for the $In_{0.53}Ga_{0.47}As$ absorber/$Al_{0.48}In_{0.52}As$ extraction barrier configuration. The excitation with high energy (blue), and lower energy (IR), illumination is also shown providing examples of the position of the photogenerated carrier in the InGaAs Γ-valley with respect to the top AlInAs barrier. (b) Temperature dependent *J*–*V* measurements from 80 K to 300 K under 1-Sun AM-1.5G excitation.

the band alignment for this proposed "proof of concept" device is shown.

Although—in principle—carriers scattered into the L valleys of the InGaAs absorber are resonant with the AlInAs extraction barrier, the mismatch in the valley degeneracy across this interface (L → Γ) results in a barrier to hot carrier extraction. This is the same physics that facilitates carrier scattering from the Γ to the L valleys in the InGaAs in the first place, and the subsequent required back transfer across the interface inhibits collection due to the lower scattering rates across the interface. The net result is thought to be a buildup of the photoelectrons at the interface where they relax to the Γ valley and result in enhanced photoluminescence and a reduction in the V_{OC} of the device.[39] A full analysis and

discussion of the effects of illumination and temperature on such devices is described more fully elsewhere.[39]

The barrier manifests itself in the presence of a strong inflection point, and therefore poor fill factor (FF), in the current density–voltage measurement under illumination. This is shown for 1-Sun, AM 1.5G, illumination as a function of the lattice temperature in Fig. 4(b). At low temperature (80 K), this barrier inhibits carrier extraction particularly at the upper InGaAs/InAlAs interface until a reverse bias of approximately −0.5 V is applied. This reverse bias likely facilitates tunneling through the barrier.[38] The thermionic emission rate across this barrier increases with increasing temperature, which coupled with the increased thermal energy of the carriers, decreases the effective band offset at the interface to ∼0.1 eV under 1-Sun illumination at 300 K.

While photogenerated carriers absorbed in the $In_{0.53}Ga_{0.47}As$ with energies lower than the $In_{0.52}Al_{0.48}As$ bandgap (∼1.5 eV) might be expected to be the source of the large loss in FF in the temperature dependent curves of Fig. 4(b), strong evidence exists that this barrier is effective to both high and low (excess) energy photogenerated carriers. This indicates that the simple potential offsets in the structure do not represent the greatest loss for the hot carrier extraction for this structure. Evidence for this is shown in Figs. 5(a) and 5(b), which illustrates the power dependent current density for monochromatic laser illumination for high (442 nm) and low (1064 nm) energy photons, respectively. These data are from the same device as assessed in Fig. 4, where the relative energy positions of this illumination was given by blue and brown arrows. From Fig. 4(a), it is clear that blue excitation will pump

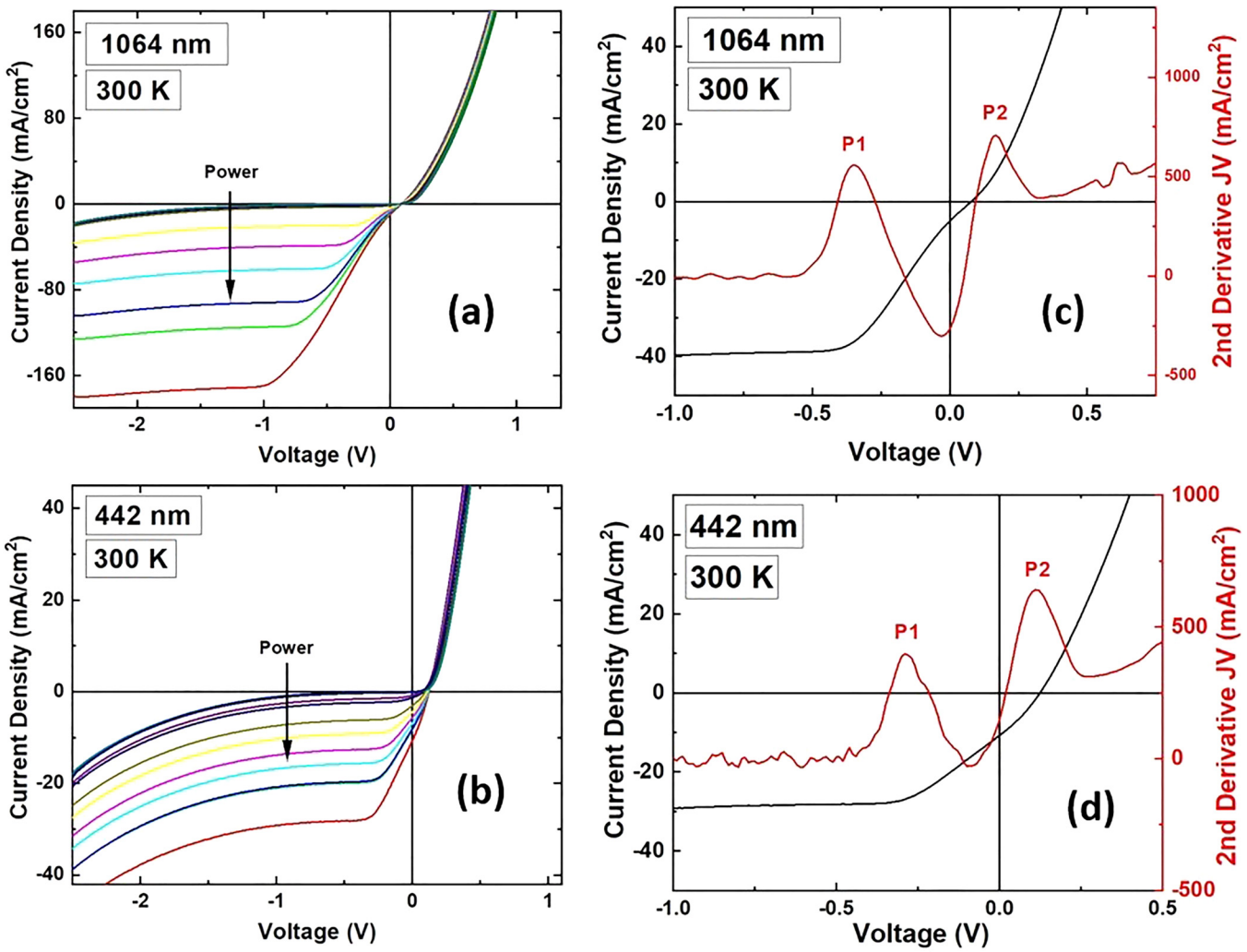

FIG. 5. Power dependent *J–V* measurements at 300 K under monochromatic illumination at (a) 1064 nm and (b) 442 nm. Comparison of monochromatic *J–V* (black) and the second derivative of the same *J–V* response (red) for the same absorbed power for (c) IR 1064 nm and (d) blue 442 nm excitation, respectively. P1 and P2 show evidence of two barriers to carrier transport within the structure.

carriers to high energy levels in the Γ valley of the InGaAs, well above the minimum of the L valleys. This will facilitate intervalley transfer of the photogenerated carriers.[11,39]

In the case of the infrared excitation, however, the photogenerated carriers are excited in the Γ valley at an energy level below the L valley minimum, and are therefore *not* scattered immediately to the upper valleys. Rather, these low energy carriers are transferred to the L valleys upon acceleration to energies sufficient for intervalley transfer; this arises from both the depletion electric field in the InGaAs and to higher electric fields that lie at the interface between the n^+ InAlAs and the InGaAs.

Further evidence of the common origin of the barrier to the carriers excited across the spectrum is the presence of a parasitic barrier to not only the 1-Sun illumination but also to the laser generated carriers, excited both below and (importantly) above the L valleys. In all cases, a power dependent barrier is observed in the fourth quadrant of the *J*–*V* curves. This indicates carriers absorbed well above the L valleys in the InGaAs and, above the InAlAs bandgap, are inhibited at the upper interface due to the valley disagreement discussed above. Recently, similar effects also have been observed in type-II InAs/AlAsSb quantum wells.[40]

To further investigate the nature of the inflection point and reduced FF in the *J*–*V* response, second derivative analysis from the illuminated *J*–*V* curves is shown in Figs. 5(c) and 5(d). This provides information on the relative change in the charge and conductivity in the device as a function of the applied voltage. Large peaks (P1, P2) indicate significant changes to the transport due to the presence of barriers arising from the positive and negative charge accumulations. These data are shown for the same monochromatic illumination as for Figs. 5(a) and 5(b) and for a photocurrent of ∼20 mA/cm^2. The multiple peaks and valleys of the second derivative curves indicate a complicated charge variation near this interface, whose origin is ascribed to the charge buildup mentioned earlier.

While P1 is ascribed to the upper interface, P2 is attributed to the sizable band offset (∼0.25 eV) in the valence band at the *n*-InGaAs/*p*-InAlAs interface, which provides a small barrier to the photogenerated holes traveling into the *p*-InAlAs. The presence of these barriers, along with the near total absorption of the illumination above 1.5 eV, shown in Fig. 2(b), removes any discussion that the large inflection in the *J*–*V* response of the device could be attributed to an unintentional *p*–*n* junction formed at the back of the device.

IV. DISCUSSION

In Secs. III A–III C, we have discussed the concept of valley photovoltaics for use in HCSCs. The original idea was to use the *p*–*n* junction described in Sec. II B, along with a top n^+ InAlAs extraction layer. Unfortunately, this structure did not prove to be as useful as predicted. As we have discussed, although this first device demonstrated the important role of the upper valleys for hot carrier transfer and storage, this initial device suffered from a barrier to extraction of the hot carriers.[39] This extraction layer also provided the semi-infinite barrier that allows only the hot carriers to be collected.[5,9] Since the early device, several alternate approaches to the extraction layer have been discussed.[41] Before discussing one of these newly proposed structures, we want to discuss other aspects of HCSCs.

A. Temperature

In much of the discussion about the physics of solar cells, there appears a considerable focus on thermalization, MB distributions, and resulting high temperatures for the carriers in these cells. In the previously mentioned Monte Carlo simulations,[11] the carriers in the L valleys were studied to ascertain their distribution function in order to estimate a temperature. This is done for an InGaAs absorber for an electric field of 12 kV/cm, which is in the range within the device discussed above, and is shown in Fig. 6. From such a plot, we can estimate an effective temperature of about 500 K; but care has to be taken with this, as it is extracted from the energy dependence of the carrier density, not from any quantity that truly represents a temperature. The problem arises as it is known that the distribution function will elongate along the electric field, which means that the temperature along the field will be higher than that normal to the field. Hence, the distribution is quite non-thermal in nature, and the use of such a temperature can be misleading.

The important point is that the actual distribution shows that the carriers are spread out over an energy range of more than 200 meV. Nevertheless, these carriers are at a relatively low "temperature." Trying to extract carriers from this distribution with a narrow-band, energy-selective filter still will collect only a small fraction of the total distribution. This supports the use of the semi-infinite barrier, in which a wide range of carrier energies above a cutoff is gathered by the extraction layer. Such a system also is

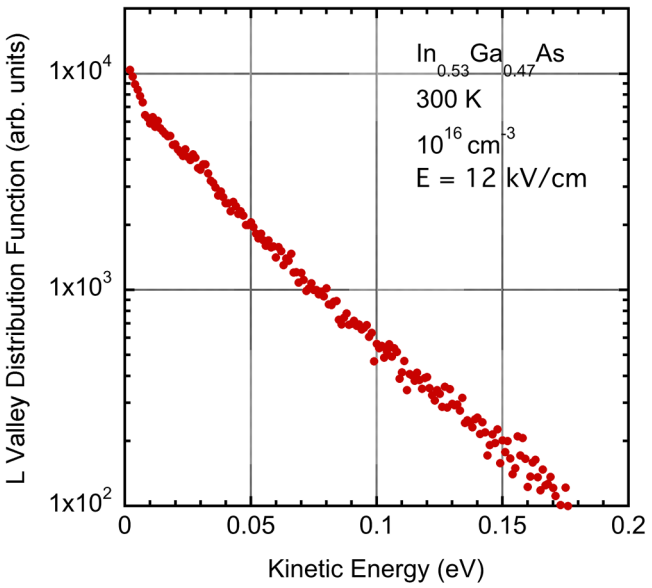

FIG. 6. The distribution function for the carriers in the L valleys of the InGaAs at an electric field of 12 kV/cm. Using the slope of this curve, we can estimate an electron temperature of ∼500 K.

much more practical to implement in a solar cell structure. The cutoff energy assures that no carriers from the Γ valley are extracted and the voltage of the solar cell is defined by the upper valleys rather than the bandgap of the absorber.

B. An improved architecture: Toward enhanced hot carrier extraction

The experiments described clearly showed that the extraction layer of the HCSC needs to be chosen with more insight. One example that has been discussed is to replace the n^+ InAlAs layer with an n^+ $GaAs_{0.51}Sb_{0.49}$ layer.[41] Empirical pseudopotential calculations show that the separation between the Γ and L valleys in GaAsSb is very small and may be only about 0.1 eV in the alloy.[42] It is known that GaSb containing compounds tend to have a band offset that gives a staggered band lineup in heterostructures with, for example, InGaAs. Importantly, this heterostructure also can be grown relatively easily,[43,44] which increases its potential for a valley photovoltaic HCSC.

As a result of the staggered alignment, it is thought that the conduction band of the GaAsSb will lie about 0.36–0.4 eV above that of the InGaAs, as shown in Fig. 7, but this is enough to obstruct carriers in the latter's Γ valley from being extracted. The L valleys in InGaAs lie about 0.5 eV above the Γ valley. Using the offset at the heterojunction and the valley separation in GaAsSb puts the L valleys of the extraction layer about 50 meV *below* those of the absorbing InGaAs layer, but close to the L valley in the 25 nm n^+-layer. This suggests that this cell structure may be effective at getting the photoelectrons out of the absorber by removing the barrier at the interface. One significant advantage of this choice of extraction layer is the fact that both the InGaAs absorber and the GaAsSb extraction layer are lattice matched to the InP substrate.

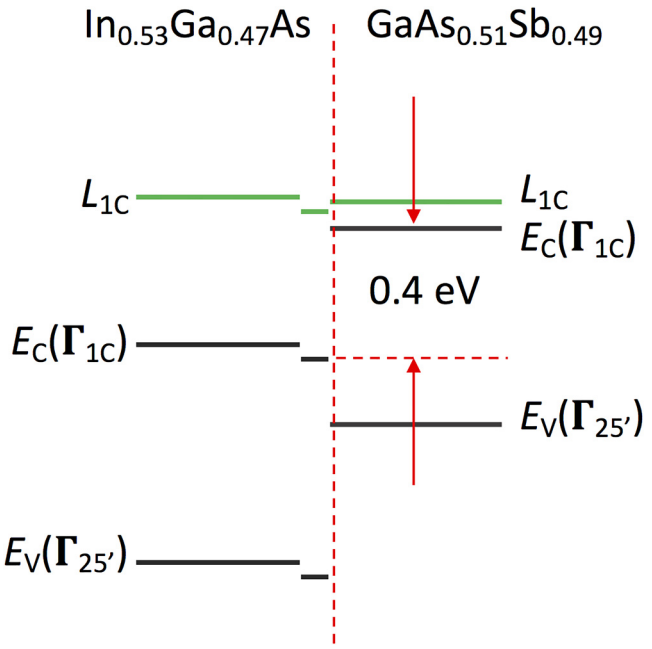

FIG. 7. Band lineup for the extraction layer of $GaAs_{0.51}Sb_{0.49}$ on top of the $In_{0.53}Ga_{0.47}As$. The heavily doped, field termination layer of the latter material is shown just to the left of the heterojunction.

V. CONCLUSIONS

Third generation cells, especially hot carrier solar cells, need to operate in a far-from-equilibrium steady state that calls into question certain assumptions that underline the Shockley–Queisser detailed balance approach. Several aspects such as high electric fields at interfaces, scattering to upper valleys, e–e scattering rates, and e–h recombination all need to be carefully considered.

Here, the idea that a practical hot carrier solar cell can be created only by utilizing the higher lying satellite valleys of the conduction band, as earlier proposed, has been discussed. By encouraging the photoelectrons to transfer to the satellite valleys, the concept originally proposed by Ross and Nozik of preventing the loss of energy through emission of optical phonons, thereby keeping the photoexcited carriers at higher energies in the conduction band can be achieved easily.[9] The use of a semi-infinite (in energy) collector layer by which all carriers above the L minimum can be collected in a manner that rejects photogenerated carriers at lower energy in the Γ valley of the absorber layer also achieves the second requirement of these latter authors.[9]

While the initial devices investigated for upper valley considerations demonstrated hot carrier transfer and storage in the L valley of the absorber and the potential of this process for third generation PV, they also suffered from a barrier to extraction of the hot carriers; therefore, high efficiency was not realized from these initial systems.[39,45] The role of the extraction layer, while further demonstrating the importance of valley scattering processes in "proof of principle" schemes, currently provides the limiting factor in the realization of an efficient valley photovoltaic device. To address this barrier problem, a different material for the extraction layer, one with a more suitable band alignment, has been proposed.

Finally, we summarize with the view that the use of the satellite valleys offers a new approach to the creation of hot carrier solar cells. By clever adjustment of various satellite valleys throughout the various layers of the cell, one achieves a novel set of pathways for extraction of the photo-carriers and reduces the amount of phonon loss within the cell. These higher energy carrier extraction pathways may be a route to a more efficient cell.

ACKNOWLEDGMENTS

The authors have benefited from useful discussions with C. Honsberg, N. J. Ekins-Daukes, and J. J. Kirch. H. Esmaielpour and K. R. Dorman are thanked for their work in processing and measuring the devices discussed in this work and M. B. Santos for MBE growth at OU. The work at OU was partially supported by the National Science Foundation ECCS Program (Grant No. ECCS-1610062). The work at ASU was partially supported by the Engineering Research Center Program of the National Science Foundation and the Office of Energy Efficiency and Renewable Energy of the Department of Energy under NSF Cooperative Agreement No. EEC-1041895. The work at OU was performed

under the umbrella of the Oklahoma Photovoltaics Research Institute (OKPVRI) and the Center for Quantum Research and Technology (CQRT) at the University of Oklahoma. Any opinions, findings, and conclusions or recommendations expressed in this material are those of the author(s) and do not necessarily reflect those of the National Science Foundation or Department of Energy.

DATA AVAILABILITY

The data that support the findings of this study are available from the corresponding author upon reasonable request.

REFERENCES

[1]E. Bequerel, Comp. Rend. **9**, 561 (1839).
[2]C. E. Fritts, Am. J. Sci. **s3-26**, 465 (1883).
[3]R. S. Ohl, U.S. patent 2,402,662 (25 June 1946).
[4]D. M. Chapin, C. S. Fuller, and G. L. Pearson, J. Appl. Phys. **25**, 676 (1954).
[5]S. M. Goodnick, C. Honsberg *et al.*, in *Springer Handbook of Semiconductor Devices*, edited by R. Brunetti (Springer-Verlag) (in press).
[6]A. Y. Ali and K. W. Böer, Sol. Cells **21**, 263 (1987).
[7]C. E. Backus, IEEE Spectr. **17**(2), 34 (1980).
[8]L. C. Hirst *et al.*, Prog. Photovolt. Res. Appl. **19**, 286 (2011).
[9]R. T. Ross and A. J. Nozik, J. Appl. Phys. **53**, 3813 (1982).
[10]M. A. Green, *Third Generation Photovoltaics: Advanced Solar Energy Conversion* (Springer, Berlin, 2003).
[11]D. K. Ferry, Semicond. Sci. Technol. **34**, 044001 (2019).
[12]P. Würfel, A. S. Brown, T. E. Humphrey, and M. A. Green, Prog. Photovolt. Res. Appl. **13**, 277 (2005).
[13]W. Shockley and H. J. Quiesser, J. Appl. Phys. **32**, 510 (1961).
[14]F. Williams and A. J. Nozik, Nature **271**, 137 (1978).
[15]J. F. Guillemoles *et al.*, Nat Photonics **13**, 501 (2019).
[16]S. Adachi, *Physical Properties of III-V Semiconductor Compounds* (John Wiley, New York, 1982).
[17]U. Rau, Phys. Rev. B **76**, 085303 (2007).
[18]I. R. Sellers *et al.*, Electron. Lett. **40**, 1412 (2004).
[19]D. K. Ferry, *Semiconductors: Bonds and Bands*, 2nd ed. (IOP Publishing, Bristol, 2020).
[20]See www.ioffe.ru/SVA/NSM/Semicond/GaInAs/ provides a variety of materials data on many semiconductors.
[21]H. Sakaki, Jpn. J. Appl. Phys. **28**, L314 (1989).
[22]D. C. Edelstein, C. L. Tang, and A. J. Nozik, Appl. Phys. Lett. **51**, 48 (1987).
[23]J. Garg and I. R. Sellers, Semicond. Sci. Technol. **35**, 044001 (2020).
[24]P. Lugli and S. M. Goodnick, Phys. Rev. Lett. **59**, 716 (1987).
[25]W. Liang *et al.*, Appl. Phys. Lett. **83**, 1438 (2003).
[26]J. S. Ayubi-Moak *et al.*, IEEE Trans. Electron Devices **54**, 2327 (2007).
[27]J. A. R. Dimmock *et al.*, Prog. Photovolt. Res. Appl. **22**, 151 (2014).
[28]C. J. Hearn, Proc. Phys. Soc. **86**, 881 (1965).
[29]D. K. Ferry, S. M. Goodnick, and K. Hess, Physica B **272**, 538 (1999).
[30]S. M. Goodnick and P. Lugli, Phys. Rev. B **37**, 2578 (1988).
[31]I. Konovalov, V. Emelianov, and R. Linke, Sol. Energy **111**, 1 (2015).
[32]I. Konovalov and B. Ploss, Sol. Energy **185**, 59 (2019).
[33]This plot is made using the NRL heterostructure bands software.
[34]H. Ono, S. Taniguchi, and T. Suzuki, Jpn. J. Appl. Phys. **43**, 2259 (2004).
[35]S. Datta *et al.*, IEEE Trans. Electron Devices **45**, 1634 (1998).
[36]K. Tateno and C. Amano, J. Cryst. Growth **220**, 393 (2000).
[37]M. J. Martinez *et al.*, J. Appl. Phys. **77**, 661 (1995).
[38]H. Taguchi *et al.*, Jpn. J. Appl. Phys. **45**, 8549 (2006).
[39]H. Esmaielpour *et al.*, Nat. Energy **5**, 336 (2020).
[40]V. R. Whiteside *et al.*, Semicond. Sci. Technol. **34**, 094001 (2019).
[41]D. K. Ferry *et al.*, in *Proceedings of the Photovoltaic Specialist Conference* (IEEE, 2020).
[42]E. Tea and F. Aniel, J. Appl. Phys. **109**, 033716 (2011).
[43]H. Detz *et al.*, J. Vac. Sci. Technol. B **28**, C3G19 (2010).
[44]Y.-C. Wu *et al.*, Semiconductors **49**, 254 (2015).
[45]G. Conibeer, Nat. Energy **5**, 280 (2020).